Transport of Pollutant in Shallow Water : A Two Time Steps Kinetic Method

Emmanuel Audusse, Marie-Odile Bristeau

INRIA

INSTITUT NATIONAL DE RECHERCHE EN INFORMATIQUE ET EN AUTOMATIQUE

Transport of Pollutant in Shallow Water A Two Time Steps Kinetic Method

Emmanuel Audusse - Marie-Odile Bristeau

No 4529

Aout 2002

THEME 4

ISSN 0249-6399 ISRN INRIA/RR--4529--FR+ENG

INRIA
ROCQUENCOURT

Transport of Pollutant in Shallow Water
A Two Time Steps Kinetic Method

Emmanuel Audusse* , Marie-Odile Bristeau †

Thème 4 — Simulation et optimisation
de systèmes complexes
Projet M3N

Rapport de recherche n° 4529 — Aout 2002 — 41 pages

Abstract: The aim of this paper is to present a finite volume kinetic method to compute the transport of a passive pollutant by a flow modelled by the shallow water equations using a new time discretization that allows large time steps for the pollutant computation. For the hydrodynamic part the kinetic solver ensures - even in the case of a non flat bottom - the preservation of the steady state of a lake at rest, the nonnegativity of the water height and the existence of an entropy inequality. On an other hand the transport computation ensures the conservation of pollutant mass, a nonnegativity property and a maximum principle for the concentration of pollutant and the preservation of discrete steady states associated with the lake at rest equilibrium. The interest of the developped method is to preserve these theoretical properties with a scheme that allows to disconnect the hydrodynamic time step - related to a classical CFL condition - and the transport one - related to a new CFL condition - and further the hydrodynamic calculation and the transport one. The CPU time is very reduced and we can easily solve different transport problems with the same hydrodynamic solution without large storage. Moreover the numerical results exhibit a better accuracy than with a classical method especially when using 1D or 2D regular grids.

Key-words: shallow water equations, Saint-Venant system, finite volume method, kinetic scheme, transport of pollutant, time discretization

* INRIA, Projet M3N, Domaine de Voluceau 78153 Le Chesnay France, Emmanuel.Audusse@inria.fr
† INRIA, Projet M3N, Domaine de Voluceau 78153 Le Chesnay France, Marie-Odile.Bristeau@inria.fr

Unit de recherche INRIA Rocquencourt
Domaine de Voluceau, Rocquencourt, BP 105, 78153 Le Chesnay Cedex (France)
Tlphone : +33 1 39 63 55 11 - Tlcopie : +33 1 39 63 53 30

Transport de polluant dans les équations de Saint-Venant
Une méthode cinétique à deux pas de temps

Résumé : L'objet de ce rapport est la résolution de certains problèmes de transport de polluant en eaux peu profondes par une méthode de volumes finis à deux pas de temps basée sur une interprétation cinétique des équations de Saint-Venant avec bathymétrie. L'intérêt de cette nouvelle méthode est d'assurer la préservation au niveau discret de nombreuses propriétés des équations hydrodynamiques - positivité de la hauteur d'eau, conservation de l'équilibre d'un lac au repos et existence d'une inégalité d'entropie - et de l'équation de transport du polluant - positivité et principe du maximum pour la concentration du polluant, conservation des équilibres liés au cas d'un lac au repos - tout en permettant de découpler - dans une certaine mesure - la résolution du problème de transport des calculs hydrodynamiques. Ainsi l'introduction d'une nouvelle condition de CFL sur l'équation de transport autorise l'utilisation de très grands pas de temps, notamment pour les écoulements à faible nombre de Froude. Les gains en terme de temps CPU et de stockage de données sont notables. De plus les expériences numériques 1D et 2D effectuées montrent que cette nouvelle méthode donnent des résultats plus précis qu'une méthode cinétique classique.

Mots-clés : équations de Saint-Venant, eaux peu profondes, volumes finis, schéma cinétique, transport de polluant, discrétisation en temps

1 Introduction

The shallow water equations are an usual model to describe the flows in rivers or coastal areas. The conservative form is written as a first order hyperbolic system with source terms coming from the bottom topography or the friction on the bed river. Research on solution methods for these equations has received considerable attention in the past two decades and a great number of finite-volume schemes have been developed - refer to [8] or [12] for a detailed presentation. The finite volume method can be used on general triangular grids with a finite element data structure and preserves the conservativity property of the equations. It requires to compute the fluxes at the control volume interface and its stability requires some upwinding in the interpolation of the fluxes and a CFL condition on time steps - refer to [5] for a survey of its properties.

A well-known difficulty of the Saint-Venant system is the preservation of nontrivial equilibria due to the presence of the source terms. It is a specific problem but necessary to compute realistic schemes. In the last years many authors treated this question along with an early idea of Roe [17] to upwind the source terms at the interfaces - see for instance [4], [6], [9], [11] or [13]. On an other hand the nonnegativity of the water height, especially when applications with dry areas are considered, is still a problem for several schemes.

Here we use a kinetic scheme initiated in [1] and developed in [16] and [2]. This scheme is based on a kinetic theory exposed in [15] that allows to link the shallow water equations to a kinetic equation at the microscopic level. In [1] only the homogeneous Saint-Venant system has a kinetic interpretation and the source terms are upwind at the macroscopic level. In [16] the source terms are also included in the kinetic formulation. The deduced schemes are conservative and we can prove analytically the nonnegativity of the water height and the conservation of the equilibrium for the steady state of a lake at rest. Moreover with the second scheme the numerical solutions satisfy a discrete entropy inequality. For proofs and numerical examples, see the papers cited above.

More specifically in this paper we are concerned with addressing several questions related to the advection of a pollutant in the Saint-Venant system. It is introduced with a classical transport equation on the concentration of pollutant. The pollution phenomena have today a very large audience and many industrial applications - see for instance [10] for the French electricity group EDF. Then several studies were initiated to best understand the chemical and biological background or the physical mechanisms - see for instance the study about the river Seine near Paris in [14]. But we do not find many works about the well adapted mathematical and numerical treatments. However it is an important point because the transport equation presents many properties that it would be interesting to satisfy at the discrete level. Indeed as for the water height we must ensure the nonnegativity of this concentration but also a maximum principle while keeping the conservation of pollutant. On an other hand as we do not introduce diffusion in the model we want also to preserve the steady state equilibria related to a lake at rest. Finally we use in our scheme the fact

that the characteristic velocities of the hydrodynamic and transport phenomena can be very different in order to disconnect the two time discretizations. It allows a larger time step for pollutant transport based upon the CFL condition

$$|u|\Delta t \leq \Delta x$$

which does not take into account the speed of sound by opposition to the hydrodynamic CFL. It is particularly useful when numerous pollutant are computed or when different pollutant problems are computed with the same hydrodynamic background as it appears often in water quality questions.

The outline of this paper is the following. After presenting the equations in Section 2, we briefly recall the kinetic formulation, the deduced scheme and its extension to the advection equation in section 3. Then we prove in Section 4 the nonnegativity properties, the maximum principle for the pollutant and the preservation of equilibria. Finally in Section 5 we present a two time steps scheme and the associated time discretization. In Section 6 we present some numerical results to illustrate the improvements of the method. Then in Section 7 we discuss an extension to the two dimensional case and we present some numerical results on realistic geometries.

2 Equations

The one dimensional shallow water system allows to describe the flow in an ideal rectangular river, at time $t \in \mathbb{R}_+$ and at the point $x \in \mathbb{R}$, through the water height $h(t,x) \in \mathbb{R}_+$ and the velocity $u(t,x) \in \mathbb{R}$, by the hyperbolic system

$$\frac{\partial h}{\partial t} + \frac{\partial (hu)}{\partial x} = S, \tag{1}$$

$$\frac{\partial (hu)}{\partial t} + \frac{\partial}{\partial x}(hu^2 + \frac{gh^2}{2}) + gh\frac{\partial z}{\partial x} = 0, \tag{2}$$

with g the gravity acceleration and $z(x) \in \mathbb{R}$ the bottom topography. Therefore $h+z$ is the level of water surface. In the following we denote $q = hu$ the discharge.
These equations were originally written by Saint-Venant in [18]. Gerbeau and Perthame present in [7] a derivation from the Navier Stokes system. The system (1)-(2) corresponds to a very simple case. Other terms can be added in the right hand side, in order to take into account frictions on the bottom or other phenomena.

To perform the analysis of transport of pollutant in this ideal river, we add a third equation

$$\frac{\partial (hT)}{\partial t} + \frac{\partial (huT)}{\partial x} = T_S S, \tag{3}$$

where $T(t,x) \in \mathbb{R}_+$ is the concentration of pollutant and T_S are the given values of the concentration of pollutant at the sources S. In the following we denote $e = hT$ the quantity of pollutant in the flow.
We can also write this equation on the nonconservative form where 'monotonicity' is better seen

$$\frac{\partial T}{\partial t} + u\frac{\partial T}{\partial x} = \frac{(T_S - T)S}{h}.$$

It is a classical transport equation. Here we suppose the pollutant is passive and does not interact with the flow. But in some cases, other phenomena like sedimentation, erosion, birth or death of particles have to be considered.

We can write this system in the conservative and compact form

$$\frac{\partial U}{\partial t} + \frac{\partial F(U)}{\partial x} = B(U), \tag{4}$$

with

$$U = \begin{pmatrix} h \\ q \\ e \end{pmatrix}, \quad F(U) = \begin{pmatrix} q \\ \frac{q^2}{h} + \frac{gh^2}{2} \\ \frac{qe}{h} \end{pmatrix}, \quad B(U) = \begin{pmatrix} S \\ -gh\frac{\partial z}{\partial x} \\ T_S S \end{pmatrix}.$$

3 The kinetic scheme

3.1 Kinetic interpretation of the shallow water equations

We introduce here a kinetic approach to system (1)-(3) written with S=0. Then we can deduce from the discretization of the kinetic equation a "kinetic scheme" for the macroscopic system.
Let $\chi(w)$ be an even and compactly supported probability defined on $\mathbb{R}$ satisfying that its second moment is equal to one. Then we introduce two microscopic densities of particles $M(t,x,\xi)$ and $N(t,x,\xi)$ defined by a Gibbs equilibrium

$$M(t,x,\xi) = \frac{h(t,x)}{c(t,x)}\chi(\frac{\xi - u(t,x)}{c(t,x)}), \tag{5}$$

$$N(t,x,\xi) = \frac{e(t,x)}{c(t,x)}\chi(\frac{\xi - u(t,x)}{c(t,x)}), \tag{6}$$

with

$$c(t,x)^2 = \frac{gh(t,x)}{2}.$$

We denote

$$G(t,x,\xi) = \begin{pmatrix} M(t,x,\xi) \\ N(t,x,\xi) \end{pmatrix}. \tag{7}$$

Theorem 3.1 *The functions (h,q,e)(t,x) are strong solutions of the shallow water system (1)-(3) if and only if $G(t,x,\xi)$ is solution of the kinetic equation*

$$\frac{\partial G}{\partial t} + \xi\frac{\partial G}{\partial x} - g\frac{\partial z}{\partial x}\frac{\partial G}{\partial \xi} = Q(t,x,\xi), \tag{8}$$

where $Q(t,x,\xi)$ is a "collision term" equal to zero at the macroscopic level.

Proof The result is obtained by a simple integration in ξ of the equation (8) against the matrix $K(\xi)$

$$K(\xi) = \begin{pmatrix} 1 & 0 \\ \xi & 0 \\ 0 & 1 \end{pmatrix}.$$

The non-linear Saint-Venant system is now reduced to a linear transport system on non-linear quantities M and N, for which it is easier to find a simple numerical scheme with good theoretical properties. For a detailed proof of the hydrodynamic part of the kinetic interpretation refer to [1] and for the treatment of the source term at this microscopic level see [16].

3.2 The kinetic scheme

We now describe the kinetic scheme without taking into account the source term due to the bottom topography. Indeed we are more interested here with the treatment of the pollutant and for the simplicity of the purpose we restrict ourselves to the flat bottom case. For a complete hydrodynamic presentation we refer to [1] or [16].

To approximate the solution $U(t,x)$, $x \in X \in \mathbb{R}$, $t \geq 0$, of the shallow water equations with transport of pollutant by discrete values U_i^n, $i \in I \subset \mathbf{Z}$, $n \in \mathbf{N}$ we consider as usual a grid of points $x_{i+1/2}$, $i \in I$,

$$\ldots < x_{i-1/2} < x_{i+1/2} < x_{i+3/2} < \ldots,$$

and we define the cells (or finite volumes) and their lengths

$$C_i =]x_{i-1/2}, x_{i+1/2}[, \qquad \Delta x_i = x_{i+1/2} - x_{i-1/2} > 0.$$

We shall denote also $x_i = (x_{i-1/2} + x_{i+1/2})/2$ and we consider a timestep $\Delta t^n > 0$ - that we will precise later - and define the discrete times by

$$t^n = \sum_0^{n-1} \Delta t^k, \quad n \in \mathbf{N}^*.$$

Now being given a piecewise constant approximation of the initial data, we must find a formula of the form

$$U_i^{n+1} = U_i^n + \sigma_i^n (F^n_{i-\frac{1}{2}} - F^n_{i+\frac{1}{2}}), \tag{9}$$

where

$$U_i^n = \begin{pmatrix} h_i^n \\ q_i^n \\ e_i^n \end{pmatrix}$$

and U_i^{n+1} are the piecewise constant approximations at times t^n and t^{n+1} on the cell C_i, σ_i^n is defined by

$$\sigma_i^n = \frac{\Delta t^n}{\Delta x_i},$$

and $F^n_{i-\frac{1}{2}}$ and $F^n_{i+\frac{1}{2}}$ must be precised.
Here we use the kinetic interpretation to precise the formula (9). First we define two discrete densities of particles $M_i^n(\xi)$ and $N_i^n(\xi)$ by

$$\begin{aligned} M_i^n(\xi) &= \frac{h_i^n}{c_i^n} \chi\left(\frac{\xi - u_i^n}{c_i^n}\right), \\ N_i^n(\xi) &= \frac{e_i^n}{c_i^n} \chi\left(\frac{\xi - u_i^n}{c_i^n}\right), \end{aligned}$$

and the corresponding quantity $G_i^n(\xi)$. Then we define a new density function $G_i^{n+1}(\xi)$ at time t^{n+1} with applying a simple upwind scheme for the discrete version of the kinetic equation (8) for every ξ and without taking account the right hand side

$$G_i^{n+1}(\xi) = G_i^n(\xi) - \xi\sigma_i^n \left(G^n_{i+\frac{1}{2}}(\xi) - G^n_{i-\frac{1}{2}}(\xi) \right),$$

with

$$G^n_{i+\frac{1}{2}}(\xi) = \left\{ \begin{array}{ll} G_i^n(\xi) & if \quad \xi \geq 0 \\ G_{i+1}^n(\xi) & if \quad \xi < 0 \end{array} \right.$$

This new density function is not an equilibrium but thanks to the property of the right hand side of (8) we can recover the macroscopic quantity at time t^{n+1} by a simple integration in ξ. Finally we can precise the macroscopic formula (9) with

$$F^n_{i+\frac{1}{2}} = F(U_i^n, U_{i+1}^n) = F^+(U_i^n) + F^-(U_{i+1}^n), \tag{10}$$

where

$$F^-(U_i^n) = \int_{\xi \in \mathbb{R}_-} \xi K(\xi)\ G_i^n(\xi)\ d\xi, \tag{11}$$

$$F^+(U_i^n) = \int_{\xi \in \mathbb{R}_+} \xi K(\xi)\ G_i^n(\xi)\ d\xi. \tag{12}$$

A detailed expression of $F^+(U_i)$ can also be written

$$F^+(U_i) = \left(\begin{array}{c} F_h^+(U_i) \\ F_q^+(U_i) \\ F_e^+(U_i) \end{array} \right) = h_i \int_{w \geq \frac{-u_i}{c_i}} (u_i + wc_i) \left(\begin{array}{c} 1 \\ u_i + wc_i \\ T_i \end{array} \right) \chi(w) dw, \tag{13}$$

This kinetic method is interesting because it gives a very simple and natural way to propose a numerical flux through the kinetic interpretation and, if we can perform analytically the integration in (13), it is numerically powerfull because the kinetic level disappears and the scheme is written directly as a macroscopic scheme.

Notice also that according to the above derivation, the pollutant flux $F_e^+(U_i)$ that we refer to as the classical kinetic scheme and that we denote $F_{k,e}^+(U_i)$ in the following, has a very simple expression

$$F_{k,e}^{\pm}(U_i) = T_i F_h^{\pm}(U_i). \tag{14}$$

Nevertheless we will not use it in practice because of a lack of accuracy as we will show in the next Subsection.

3.3 Preservation of the equilibria

We do not treat here the problem of the hydrodynamic equilibria because in the case of a flat bottom they are trivially preserved. We refer to [1] or [16] where the authors prove analytically the preservation of the lake at rest equilibrium whatever is the bottom topography.

We are now interested with the problem of the conservation of equilibria for the pollutant. Consider the situation of a lake at rest - with a flat bottom or not - and a numerical scheme that preserves it. Then the numerical discharge vanishes and the water height is constant. So

$$F_h(U_j, U_{j+1}) = 0 \quad \forall\, j \in \mathbf{Z}, \tag{15}$$

and so due to (10)

$$F_h^+(U_j) = -F_h^-(U_{j+1}) \quad \forall\, j \in \mathbf{Z},$$

but - from (13) - these two fluxes are not equal to zero.
Now put some pollutant with concentration equal to one at the node i of the mesh and zero everywhere else. As there is no diffusion in the model this situation is an equilibrium. But numerically - from (14) - the classical kinetic scheme induces

$$F_{k,e}^{\pm}(U_i) \neq 0,$$
$$F_{k,e}^{\pm}(U_j) = 0 \qquad \forall\, j \neq i,$$

and then (10) shows immediately that the equilibrium is not preserved for the concentration of pollutant. For long time integration the classical kinetic scheme will create very large diffusion for the pollutant and thus we discard it.

We rather introduce some upwinding in the transport advection depending on the sign of the total mass flux. Then the pollutant flux vanishes with the total mass flux. It is done with the introduction of the new pollutant flux $F_{uk,e}(U_i, U_{i+1})$ defined in the following formula that replaces (14)

$$F_{uk,e}(U_i, U_{i+1}) = T_{i+\frac{1}{2}} F_h(U_i, U_{i+1}) \tag{16}$$

where

$$T_{i+\frac{1}{2}} = \begin{pmatrix} T_i & for \quad F_h \geq 0, \\ T_{i+1} & for \quad F_h \leq 0. \end{pmatrix} \tag{17}$$

In the following we call this new scheme the upwind kinetic scheme.

Theorem 3.2 *With the pollutant flux (16)-(17) the upwind kinetic scheme (9)-(12) preserves the pollutant equilibrium in a lake at rest.*

Proof The hydrodynamic computation is unchanged and so (15) is always true. Then from (16)-(17) we have immediately

$$F_{uk,e}(U_j, U_{j+1}) = 0 \quad \forall\, j \in \mathbf{Z}.$$

4 Properties of the scheme

4.1 Positivity of the water height

In addition to the preservation of the hydrodynamic and transport equilibria in a lake at rest the upwind kinetic scheme has numerous good properties. As we are interested here with the coupling between the shallow water system and a transport equation, the problem of the source term is not treated. As for the hydrodynamic part of the proofs we restrict ourselves to the case of a flat bottom. But notice that these results also hold true with a non-flat bottom, cf [1] or [16] for complete proofs on the hydrodynamic part. In Sections 6 and 7 some numerical examples with a non-flat bottom are presented using our scheme.

Theorem 4.1 *The scheme is consistent and conservative. It ensures the nonnegativity of the water height under the CFL condition*

$$\Delta t^n \leq min\left(\frac{\Delta x_i}{|u_i^n| + w_M c_i^n}\right). \tag{18}$$

where $2w_M$ is the size of the compact support of χ.

Proof Consistency and conservativity are easily deduced by (9)-(12).
To prove the positivity of the water height let us go back to the microscopic level. Suppose we have $h_i^n \geq 0\ \forall i \in \mathbf{Z}$. From the definition of the function M in (5) and the positivity of the function χ, we immediately deduce

$$M_i^n(\xi) \geq 0 \qquad \forall i.$$

We now introduce the quantities ξ_+, ξ_- defined by

$$\xi_+ = \max(0, \xi), \quad \xi_- = \max(0, -\xi), \tag{19}$$

and so we write the upwind microscopic scheme deduced by (8) in the form

$$f_i^{n+1}(\xi) = (1 - \sigma_i^n|\xi|)M_i^n(\xi) + \sigma_{i-1}^n \xi_+ M_{i-1}^n(\xi) + \sigma_{i+1}^n \xi_- M_{i+1}^n(\xi). \tag{20}$$

Then, for each j, either the value of ξ is such that

$$|\xi - u_j^n| \geq w_M c_j^n,$$

and then from the definitions of w_M and of function M we have

$$M_j^n(\xi) = 0,$$

or the value of ξ is such that

$$|\xi - u_j^n| \leq w_M c_j^n,$$

which implies that $|\xi| \leq (|u_j^n| + w_M c_j^n)$ and then, using the CFL condition (18), we obtain

$$\sigma_j^n |\xi| \leq 1.$$

Therefore in the relation (20), $f_i^{n+1}(\xi)$ is a convex combination of nonnegative quantities and thus

$$f_i^{n+1}(\xi) \geq 0.$$

With a simple integration in ξ, we obtain

$$h_i^{n+1} \geq 0.$$

4.2 Positivity of the concentration of pollutant

Theorem 4.2 *The upwind kinetic scheme (9)-(12) and (16)-(17) preserves the positivity of the concentration of pollutant.*

Proof We present first another equivalent formula for the pollutant flux (16)-(17)

$$F_{uk,e}(U_i, U_{i+1}) = T_i F_h(U_i, U_{i+1})_+ - T_{i+1} F_h(U_i, U_{i+1})_-, \tag{21}$$

where we refer to (19) for the definitions of the positive and negative parts.
We assume that the concentration of pollutant is nonnegative at time t^n and we drop the superscripts n for simplicity. Then

$$(hT)_i^{n+1} = (hT)_i + \sigma_i \left(F_{uk,e}(U_{i-1}, U_i) - F_{uk,e}(U_i, U_{i+1}) \right),$$

that is exactly with (21)

$$\begin{aligned} (hT)_i^{n+1} &= (hT)_i \\ &+ \sigma_i [T_{i-1} F_h(U_{i-1}, U_i)_+ - T_i F_h(U_{i-1}, U_i)_- \\ &\quad - T_i F_h(U_i, U_{i+1})_+ + T_{i+1} F_h(U_i, U_{i+1})_-]. \end{aligned} \tag{22}$$

Thanks to the nonnegativity of the concentration of pollutant at time t^n we can write the inequality

$$(hT)_i^{n+1} \geq T_i \left(h_i - \sigma_i \left(F_h(U_{i-1}, U_i)_- + F_h(U_i, U_{i+1})_+ \right) \right). \tag{23}$$

Now we remark from (11)-(12) and due to the positivity of function M that

$$\begin{aligned} F^-(U_j) \leq 0 \quad \forall\, j \in \mathbf{Z}, \\ F^+(U_j) \geq 0 \quad \forall\, j \in \mathbf{Z}, \end{aligned}$$

and so we can write, using (10),

$$(hT)_i^{n+1} \geq T_i \left(h_i - \sigma_i \left(F_h^+(U_i) - F_h^-(U_i) \right) \right).$$

Until now we have not used the fact that we are on a flat bottom and if we forget the concentrations of the pollutant in the precedent expression we recognize a step of the proof of the nonnegativity of the water height. We can conclude the two proofs are linked and so if the scheme ensures the nonnegativity of the water height then it ensures automatically the nonnegativity of the concentration of pollutant - whatever is the form of the bottom. More precisely in the case of a flat bottom the end of the proof is to use the detailed expression of the fluxes to minimize the right hand side. Indeed from (13) and thanks to the property of χ

$$\begin{aligned} F_h^+(U_i) - F_h^-(U_i) &= h_i \int_{w \geq \frac{-u_i}{c_i}} (u_i + w c_i)\chi(w)dw \\ &\quad - h_i \int_{w \leq \frac{-u_i}{c_i}} (u_i + w c_i)\chi(w)dw \\ &\leq h_i \int_{w \in \mathbb{R}} (u_i + |w| c_i)\chi(w)dw \\ &\leq h_i(u_i + w_M c_i). \end{aligned}$$

Therefore, we deduce

$$(hT)_i^{n+1} \geq T_i h_i \left(1 - \sigma_i(u_i + w_M c_i)\right)$$

and the CFL condition (18) ensures also the nonnegativity of concentration of pollutant.

4.3 Maximum principle for the concentration of pollutant

Theorem 4.3 *The upwind kinetic scheme (9)-(12) and (16)-(17) ensures a maximum principle for the concentration of pollutant. Indeed it satisfies*

$$\forall n \quad \forall i \quad T_i^{n+1} \leq max(T_{i-1}^n, T_i^n, T_{i+1}^n). \tag{24}$$

Proof We rewrite (22) in another form - still dropping the superscripts n for more readability

$$\begin{aligned} (hT)_i^{n+1} &= T_i \left(h_i - \sigma_i \left(F_h(U_{i-1}, U_i)_- + F_h(U_i, U_{i+1})_+\right)\right) \\ &\quad + T_{i-1}\sigma_i F_h(U_{i-1}, U_i)_+ + T_{i+1}\sigma_i F_h(U_i, U_{i+1})_-. \end{aligned} \tag{25}$$

The two last parts of the right hand side are clearly nonnegative and we established in the precedent proof it is true for the first part too. So we can maximize the left quantity

$$\begin{aligned} (hT)_i^{n+1} \leq \quad & max\left(T_{i-1}, T_i, T_{i+1}\right) \\ & \left(h_i + \sigma_i(-F_h(U_{i-1}, U_i)_- - F_h(U_i, U_{i+1})_+ \right. \\ & \left. + F_h(U_{i-1}, U_i)_+ + F_h(U_i, U_{i+1})_-)\right). \end{aligned}$$

A simple reorganization of the right hand side gives with the formulae (9) and (10)

$$(hT)_i^{n+1} \leq h_i^{n+1} max\left(T_{i-1}, T_i, T_{i+1}\right).$$

5 Larger time steps for the pollutant

5.1 Motivation

It is well known that the two eigenvalues of the Saint-Venant system are related to the velocity of the flow and to the water height by the formulae $u + \sqrt{gh}$ and $u - \sqrt{gh}$. The eigenvalue of the transport equation is simply equal to the velocity of the flow. So it appears in the cases where the Froude number defined by

$$Fr = \frac{u}{\sqrt{gh}}$$

is small - that is almost always the case for a classical river - the characteristic time for information transfer is very different for the hydrodynamic and for the transport parts. Then if the CFL number is relevant for the hydrodynamic computation it is not connected to the physical background of the transport phenomenon. So it could be interesting to create an adaptive numerical scheme that allows to disconnect the two time discretizations. Especially in some realistic applications, when we can have to treat twenty or thirty different pollutants - and some of them are modeled by more complicated equations than (3) - or when we want to test different phenomena of pollution in the same hydrodynamic background. So we would like to solve only the relevant transport states and to store only the useful global hydrodynamic informations while ensuring all the properties presented in the previous section.

The way to reach our goal is to disconnect the transport solution from the CFL condition (18). Indeed this time step condition is strictly related to the eigenvalues of the hydrodynamic process but it is not necessary to ensure the transport properties. In fact it appears that the only theoretical time step restriction is given by the positivity of the right hand side of (23) - the nonnegativity property that we can then deduce is also sufficient to prove the maximum principle. It is clear that the CFL condition (18) is more restrictive. On an other hand notice that (23) is the less restrictive formula that we can obtain, if we imposed the nonnegativity condition for the concentration of pollutant at time t^{n+1} and at the node i is controlled by the concentration of pollutant at time t^n at the same node.

5.2 Algorithm

We now consider two different time step conditions. Notice that the CFL condition (18) is an a priori condition - we need only to know the hydrodynamic state at time t^n to compute the time step - when the transport time step condition (23) is an a posteriori condition - we must compute the mass fluxes before to compute the time step condition. On an other hand it is convenient to manage with the hydrodynamic and the pollutant quantities at the same time and so the transport time step must be the sum of some hydrodynamic time steps.

So we propose the following algorithm : starting from a given state we perform the hydrodynamic computation - time step and fluxes - then we compute the transport time step condition (23) with this time step and these fluxes. If (23) is satisfied we perform another hydrodynamic computation, we sum the hydrodynamic time steps and fluxes and we compute (23) with these sums. We continue this algorithm until (23) is not satisfied. Then we compute the new pollutant state.

Before we present precisely the algorithm let us make some useful remarks. First the hydrodynamic computation is exactly the same as in the case of the upwind solution. It means that our strategy preserves the fact that the pollutant has no influence on the hydrodynamic phenomena and it ensures that the positivity property is preserved. Second the transport time step is computed as a sum of hydrodynamic time steps. It means that we can not know a priori the transport time step but it allows to be very adaptive and the transport time step is as large as possible in relation to the hydrodynamic conditions. Third the reference to the transport time step condition ensures the preservation of the properties of the precedent section.

Let us now present the details of the algorithm :

Initialization

- Start from the state h_i^n, q_i^n, e_i^n.
- Initialization of the transport time step and total fluxes :

$$\begin{aligned} \Delta t^n &= 0, \\ G_h^n(U_{i-1}, U_i) &= 0, \\ G_h^n(U_i, U_{i+1}) &= 0. \end{aligned}$$

- Initialization of the step indicator :

$$k = 0.$$

- Initialization of the small time step hydrodynamic computation :

$$\begin{aligned} h_i^{n,0} &= h_i^n, \\ q_i^{n,0} &= q_i^n. \end{aligned}$$

Computation at the step n,k

1. Computation of hydrodynamic time step $\Delta t^{n,k}$ deduced by the CFL condition (18) related to $h_i^{n,k}$ and $Q_i^{n,k}$.
2. Computation of the partial fluxes $F^+(U_i)^{n,k}$ and $F^-(U_i)^{n,k}$ with the formula (13).

3. Computation of the total interfaces fluxes $F^{n,k}(U_i, U_{i+1})$ and $F^{n,k}(U_{i-1}, U_i)$ with the formula (10).

4. Test based on an extension of the nonnegativity condition (23) :

$$\begin{aligned} h_i^{n,k} &- \frac{1}{\Delta x_i}\left(\sum_0^k \Delta t^{n,j} F_h^{n,j}(U_i, U_{i+1})\right)_+ \\ &- \frac{1}{\Delta x_i}\left(\sum_0^k \Delta t^{n,j} F_h^{n,j}(U_{i-1}, U_i)\right)_- \geq 0. \end{aligned} \tag{26}$$

Updating of the solution

- If (26) is true then update the hydrodynamic quantities

$$h_i^{n,k+1} = h_i^{n,k} - \frac{\Delta t^{n,k}}{\Delta x_i}\left(F_h^{n,k}(U_i, U_{i+1}) - F_h^{n,j}(U_{i-1}, U_i)\right),$$
$$Q_i^{n,k+1} = Q_i^{n,k} - \frac{\Delta t^{n,k}}{\Delta x_i}\left(F_Q^{n,k}(U_i, U_{i+1}) - F_Q^{n,j}(U_{i-1}, U_i)\right),$$

  the transport quantities

$$G_h^n(U_{i-1}, U_i) = G_h^n(U_{i-1}, U_i) + \Delta t^{n,k} F_h^{n,j}(U_{i-1}, U_i),$$
$$G_h^n(U_i, U_{i+1}) = G_h^n(U_i, U_{i+1}) + \Delta t^{n,k} F_h^{n,k}(U_i, U_{i+1}),$$
$$\Delta t^n = \Delta t^n + \Delta t^{n,k},$$

  and the step indicator

$$k = k + 1.$$

  Then go to the **Computation** step.

- If (26) is false then update the hydrodynamic quantities

$$h_i^{n+1} = h_i^{n,k},$$
$$Q_i^{n+1} = Q_i^{n,k}.$$

  and the new concentration of pollutant

$$\begin{aligned} (hT)_i^{n+1} &= (hT)_i^n \\ &+ \frac{1}{\Delta x_i}\left(T_{i-1}\left(G_h^n(U_{i-1}, U_i)\right)_+ + T_i\left(G_h^n(U_{i-1}, U_i)\right)_-\right) \\ &- \frac{1}{\Delta x_i}\left(T_i\left(G_h^n(U_i, U_{i+1})\right)_+ + T_{i+1}\left(G_h^n(U_i, U_{i+1})\right)_-\right). \end{aligned}$$

  Then go to the **Initialization** step.

5.3 Consistency, conservativity, positivity, maximum principle and preservation of equilibria

The hydrodynamic computation is unchanged and so the scheme is still consistent and conservative for its hydrodynamic part and the nonnegativity of the water height is still ensured by the CFL condition introduced at each hydrodynamic time step.

On an other hand the consistency and the conservativity are also preserved for the transport part thanks to the form of the algorithm and the nonnegativity of the concentration of pollutant is ensured at each transport time step by the test (26). The maximum principle is satisfied too because the essential point - that is the nonnegativity of each term in equation (25) - is also ensured by the same test (26).

Finally the preservation of the different equilibria in a lake at rest is always true because even if the scheme contains now two different time discretizations its global form for hydrodynamic part on one hand and for transport part on the other hand is not modified.

6 Numerical results

6.1 Dam break

We begin with the very classical case of a dam break on a flat bottom in which the concentration of pollutant is different on each side of the dam. The geometrical and time data are the following :

Spatial domain : $x \in [-1000, 1000]$
Uniform mesh with 101 points.
Physical time : $240s$.

The hydrodynamic and pollutant data are - with the classical notations and with the subscripts l for the negative values of x and r for the positive ones

$$\begin{aligned} h_l &= 1. & h_r &= .5 \\ Q_l &= 0. & Q_r &= 0. \\ T_l &= .7 & T_r &= .5 \end{aligned}$$

The interest of this example is that we can compute the exact solution - cf [19]. Indeed the hydrodynamic solution is composed with three flat zones - the two original inactive zones at the two ends and an intermediate one - separated by two simple waves - a rarefaction wave going to the left and a shock wave going to the right. And the jump in the concentration is just transported at the speed u_i of the intermediate flat zone which is given by the relation

$$-2u_i^2 \left(c_l - \frac{u_i}{2}\right)^2 c_r^2 + \left(\left(c_l - \frac{u_i}{2}\right)^2 - c_r^2\right)\left(\left(c_l - \frac{u_i}{2}\right)^4 - c_r^4\right) = 0, \tag{27}$$

where c_l and c_r are defined by

$$c_l^2 = gh_l, \quad c_r^2 = gh_r.$$

We present in Figure 1.1 and 1.2 the water height and the discharge profiles. In Figure 1.3 are compared the exact concentration of pollutant, the results obtained with the upwind kinetic scheme and with the two time steps one. Then in Figure 1.4 we show a zoom on the discontinuous area.

In addition to this first example we present four other cases of dam break on flat bottom with different values for the concentration of pollutant on the right side of the dam.

$$\begin{aligned} \text{Extra Small jump} &: & h_l &= 1. & h_r &= .95 \\ \text{Small jump} &: & h_l &= 1. & h_r &= .8 \\ \text{Large jump} &: & h_l &= 1. & h_r &= .1 \\ \text{Extra Large jump} &: & h_l &= 1. & h_r &= .01 \end{aligned}$$

Our goal is to exhibit the autoadaptive aspect of the method in terms of ratio between the number of hydrodynamic time steps and the number of transport time steps. So we present in Figure 2 the zoom view on the discontinuous area for concentration of pollutant for the four new cases.

Thanks to these five experiences we can make some remarks : First - look on the x-coordinates in each zoom view - the speed of the pollutant shock front grows with the size of the water height jump as it is given by the formula (27) and the two schemes give the right speed. Second the two time steps solution is always better than the upwind one and the difference is more important when the jump is smaller. So the method improves not only the computation time but also the precision of the results - even if it will be less noteworthy in the case of a non uniform mesh as we will see below. Third the upwind and the two time steps solutions get closer - in the case of the extra large jump they are exactly the same - when the water height jump is larger - and so when the Froude number on the shock in the concentration of pollutant increases. This evolution is related to the last and more important point that we want to notice. To exhibit it we indicate below the number of transport time steps, the number of hydrodynamic time steps and the Froude number on the pollutant jump for each one of the five dam break test cases.

h_l	h_r	Froude number	Transport Steps	Hydrodynamic Steps
1.	.95	0.026	1	47
1.	.8	0.112	5	48
1.	.5	0.346	13	51
1.	.1	1.178	29	57
1.	.01	2.834	62	62

Table 1: Comparison between numbers of hydrodynamic and transport time steps

These results imply clearly that in the cases where the improvement on the accuracy of the results is the most important - which corresponds to the cases where the Froude number is small - the computation cost economy could also be very important because the gain in term of number of time steps is very large. It will authorize also to apply different pollution models on the same hydrodynamic background easily since we need to store only one global hydrodynamic information - which corresponds to the global mass flux at each interface - for each transport time step.

6.2 Peak in the concentration of pollutant

The goal of this example is to show that the improvement in the accuracy observed in the dam break problem can have important consequences in the case where the concentration

of pollutant has rapid oscillations.
The hydrodynamic initialization is still a dam break. The numerical values are the same as in the first example of the previous Subsection. The concentration of pollutant is still different on each side of the dam. But now there is a peak in the concentration of pollutant just before the dam. Indeed the initial value for the concentration of pollutant is

$$\begin{aligned} -1000. \leq x < -100. \quad &: \quad T(x,0) = T_l = 0.7 \\ -100. \leq x \leq 0. \quad &: \quad T(x,0) = T_i = 0.9 \\ 0. < x \leq 1000. \quad &: \quad T(x,0) = T_r = 0.5 \end{aligned}$$

We do not have an analytical solution for this case. But we know the initial value at the point $x = 0.$ will be simply transported with the speed u_i given by (27). So as we prove on an other hand a maximum principle for the concentration of pollutant we know its maximum value will stays equal to T_i.
In Figure 3 are presented the two numerical solutions after 250 seconds. We indicate the initial solution too. The differences between the two schemes are no more limited to a varying size for the diffusive area. Indeed the large diffusion of the upwind kinetic scheme conducts to loose the exact maximum value of the concentration of pollutant while the two time steps scheme computes it exactly.

6.3 Lake at rest

To begin with the numerical examples on non-flat bottom we verify numerically that a pollutant steady state related to the lake at rest equilibrium is preserved by the two schemes. So the bottom topography is given by

$$\begin{aligned} 0. \leq x < 8. \quad &: \quad Z(x) = 0. \\ 8. \leq x \leq 12. \quad &: \quad Z(x) = 0.2 - 0.05(x-10)^2 \\ 12. < x \leq 20. \quad &: \quad Z(x) = 0. \end{aligned}$$

and we use a uniform mesh with 101 points of discretization.
The water is initially at rest

$$\begin{aligned} h(x,0) &= H = 1. \\ Q(x,0) &= Q = 0. \end{aligned}$$

and we consider that some area is initially polluted

$$\begin{aligned} 0. \leq x < 8. \quad &: \quad T(x,0) = T_l = 0. \\ 8. \leq x \leq 10. \quad &: \quad T(x,0) = T_i = 1. \\ 10. < x \leq 20. \quad &: \quad T(x,0) = T_r = 0. \end{aligned}$$

The exact solution is clearly that the initial state is preserved and we proved analytically that the upwind and the two time steps schemes preserved exactly this property. We present the numerical results after 100 seconds in Figure 4. They are consistent with the theory.
Nevertheless a difference appears between the two schemes in term of number of transport time steps : while this number is related to the CFL condition for the upwind scheme and so increases with the physical time, it stays equal to one whatever the physical time is for the two time steps scheme. Indeed as the mass fluxes are equal to zero at each hydrodynamic time step the nonnegativity test (26) is always true and the end of the loop takes place at the end of the computation. So we avoid many useless computations. The consequences in term of CPU time are clear specially when there is a lot of different pollutants.
If we extend the test until very large physical time this difference has another big consequence. Indeed for physical times equal to one or two days - around one million hydrodynamic time steps with our data - the hydrodynamic quantities stay equal to their initial values but some diffusion appears in the concentration of pollutant computed by the upwind kinetic scheme. With the two time steps scheme there is still only one large transport time step and so this problem is avoided. Numerical illustrations are presented in Figure 5.

6.4 Emission of pollutant problem

Here we want to test the introduction of a source of pollutant in a stationary flow. This can model for instance the emission of waste water in a river.
We consider the same bottom profile as in the precedent case - except the length of the channel is now 1000 meters. Then there exist four different hydrodynamic stationary cases following the different fluid states - fluvial or torrential flows. See [1] or [16] for more details. Here we choose to work with the fluvial flow problem where the improvement due to the two time steps scheme is very clear because of a small Froude number.

$$h(x,0) = H = 2.$$
$$Q(x,0) = Q = 1.$$

We introduce between times t_b and t_e and at the node I_s a source of water S_s with a concentration of pollutant T_s. Then we follow the evolution of this pollutant layer. Notice that the source modifies locally in time and space the hydrodynamic computation.

$$I_s = 10, \quad S_s = .01m * s^{-1}, \quad T_s = 10.$$
$$t_b = 100s, \quad t_e = 300s$$

Numerical results are presented in Figure 6 and informations about the number of time steps are given in the next subsection.

6.5 With non uniform meshes

We first mention that the improvement of the two time steps method in term of accuracy was very related to the regularity of the mesh. Here we want to show this fact through some numerical examples on non uniform meshes.

We introduce two new meshes. The first one is a uniform mesh with some random perturbation and the second one is a totally random mesh. We use again the dam break problem with a peak in the concentration of pollutant - see subsection 6.2. We compute this test on our two new meshes and with our two methods - the upwind kinetic scheme and the two time steps kinetic scheme - and we present the results in the Figure 7 - where we recall the results with the uniform mesh too.

We first remark that more irregular is the mesh more the CFL condition is restrictive since it is related to the smallest space step. So the number of time steps and then the numerical diffusion increase with the irregularity of the mesh and the precision of the results decreases. On an other hand it appears clearly that the difference in the precision of the results between the upwind and the two time steps methods decreases when the mesh is very irregular. However the two time steps method is always more accurate than the upwind one and - that is the essential point - we show on the table below that the ratio between the number of transport and hydrodynamic time steps is independent of the regularity of the mesh. So there is always an important improvement on the computation time and on the storage.

Mesh	Transport Steps	Hydrodynamic Steps
Regular mesh	13	53
Semi-random mesh	30	148
Random mesh	158	691

Table 2: Comparison between different meshes for a dam break problem with a peak in the concentration of pollutant

Then we compute the emission of pollutant problem of the subsection 6.4. We apply the upwind and the two time steps methods on our three meshes and we present the results for two times - 350 seconds and 750 seconds - in the Figure 8. We present the informations about the number of time steps in the table below too. The conclusions are the same as for the dam break problem.

Mesh	Physical time	Transport Steps	Hydrodynamic Steps
Regular mesh	350	42	416
Regular mesh	750	89	890
Semi-random mesh	350	114	1246
Semi-random mesh	750	243	2669
Random mesh	350	564	5633
Random mesh	750	1207	12064

Table 3: Comparison between different meshes for an emission of pollutant problem

7 Extension to the 2D case

We now want to apply our new method to two-dimensional problems. We do not want to make here a complete presentation of the two dimensional finite volume method on a general triangular grid or of the general kinetic theory in 2D. We just mention that starting from a triangulation of $\mathbb{R}^2$ the dual cells C_i are obtained by joining the centers of mass of the triangles surrounding each vertex P_i. Then the general method is close to the 1D finite volume method. Indeed the fluxes which appear in the scheme are interpolations of the normal component of the fluxes on the edge of each cell. So locally the problem can be treated as a planar discontinuity and the interpolation can be performed using a one dimensional solver. For a complete presentation of the kinetic interpretation of the hydrodynamic part in 2D refer to [1] and for a presentation that includes the transport theory see [3]. Before we present the numerical results let us insist on the fact that as the 2D computation is based on a 1D strategy the properties we proved in 1D are also true for the 2D schemes. We do not reproduce the proofs here because they are easy extensions of those in Section 4.

We perform two numerical tests : first a dam break problem in a rectangular channel with a peak in the initial concentration of pollutant - see the subsection 6.2 in 1D - and then an emission of pollutant problem in a realistic river geometry.
For the dam break problem we use two meshes : a uniform one and an unstructured one. Then as in the 1D case we can compare the results based on the mesh regularity. The uniform mesh that we use has 1111 nodes and 2000 elements and the unstructured one has 1347 nodes and 2472 elements. As the dam break case is essentially a 1D problem we can also make comparisons between 1D and 2D solutions.
The realistic river case is managed only with an unstructured mesh and exhibits that our methods is well adapted to treat complex geometry since the gain on the number of time steps is even more important than for the academic problems.

7.1 A 2D dam break problem

We begin with the dam break problem. The data are the same as for the problem performed in the Subsection 6.2 except the length of the channel which is now one meter - and so the final time is only one second. The width is chosen equal to 0.1 meter.
The results are presented in Figures 9 and 10. The data are invariant in y-coordinates and so the solution is very close to a 1D solution. For each figure the blue color indicates the minimum level and the red color the maximum one.
In Figure 9 we first present the two meshes. Then we present the water height in the channel. On the left we recognize the rarefaction wave and on the right the shock wave. Then in the second subfigure the Froude number is presented. The profile is very close to the discharge profile in 1D.
Finally in the four last subfigures are presented the concentration of pollutant performed

with the upwind kinetic scheme and with the two time steps scheme on the unstructured mesh and then the same results with the uniform one. The profiles are very similar to the 1D profile. With the unstructured mesh the two profiles are very close - even if the maximum of the concentration is a little larger with the two time steps method as in the 1D computation when the mesh is irregular. With the uniform mesh the profiles are more different. With the upwind kinetic scheme the results are worse than on the unstructured mesh - because the uniform mesh has less nodes - but with the two time steps scheme the results are better than on the unstructured mesh - even if the uniform mesh has less nodes. So as in the 1D computation the improvement on the accuracy of the results is more significant when the mesh is more regular.

Before to end with this problem we make a comparison between the 1D and the 2D results. So we perform the computations with the same initial conditions and we consider the 2D results on the line y=0.5. Then we present in Figure 11 the results on the three 1D meshes and on the two 2D meshes. We can see that the regularity of the mesh has the same effects in 1D and in 2D - even if the 1D uniform mesh induces a smaller diffusion than the 2D uniform mesh.

7.2 Emission of pollutant in a realistic river

Then we perform an emission of pollutant problem in a river. The geometric data include a jetty in the transversal direction and a pillar bridge. We introduce a source of pollutant at one node of the mesh and for a given time - 1000 seconds to 1800 seconds - and we follow the evolution of the pollutant layer.

We use a second order scheme to compute the hydrodynamic part because the first order solution does not show the recirculation after the jetty which is very important to compute a realistic profile of the concentration of pollutant. We keep a first order solution for the transport part to not mix the improvement due to high order schemes and those due to the applied method. Results are presented in Figure 13. Here the mesh is unstructured and so the concentration of pollutant profiles are very close. But as in the other cases the two time steps scheme is a little bit better.

8 Conclusion

Thanks to a precise analysis of the upwind kinetic scheme we deduced a two time steps kinetic scheme that preserves the theoretical properties of the upwind kinetic scheme. By opposition to the hydrodynamic CFL condition, the new transport time step condition links automatically the transport time step, the space step and the fluid velocity, ignoring the sound speed.
The hydrodynamic part of the computation is unchanged. All the hydrodynamic information that is useful for the pollutant transport computation can be stored in global interface fluxes at each transport time step.
The developed method is very interesting for the "small Froude number" flows. Indeed the two time steps are very close when the speed of the flow is large compared with the "sound speed" but very different in the other case. As we can see on the table below, in a 2D realistic geometry and for a Froude number close to 0.1 - that is a classical order of magnitude for rivers, the new transport time step is around hundred and fifty times larger than the hydrodynamic time step issued from the CFL condition.

	Froude number	Transport Steps	Hydrodynamic Steps
Unstructured channel	0.35	28	385
Uniform channel	0.37	14	170
Realistic river	0.08	320	45637

Table 4: Comparison between numbers of hydrodynamic and transport time steps for the 2D test cases

The improvement is proved to be optimal if we want to preserve a priori the nonnegativity properties of the upwind kinetic scheme.
As the new time step condition is specifically adapted to the transport equation the numerical diffusion of the two time steps kinetic scheme is lower than the numerical diffusion of the upwind kinetic scheme and we improve the accuracy of the results.

References

[1] Audusse E., Bristeau M.O. and Perthame B., Kinetic schemes for Saint-Venant equations with source terms on unstructured grids, *INRIA Report*, RR-3989 (2000), http://www.inria.fr/RRRT/RR-3989.html

[2] Bristeau M.O. and Coussin B., Boundary conditions for the shallow water equations solved by kinetic schemes, *INRIA Report*, RR-4282 (2001), http://www.inria.fr/RRRT/RR-4282.html

[3] Bristeau M.O. and Perthame B., Transport of pollutant in shallow water using kinetic schemes, *ESAIM : Proceedings*, 10, CEMRACS (1999), 9-21, http://www.emath.fr/Maths/Proc/Vol.10.

[4] Bermudez A. and Vasquez M.E., Upwind methods for hyperbolic conservation laws with source terms, *Comput. Fluids*, **23** (1994), no. 8, 1049-1071.

[5] Eymard R., Gallouet T., Herbin R., *Finite volume methods, Handbook of numerical analysis*, vol VIII, P.G. Ciarlet and J.L. Lions editors, Amsterdam, North-Holland, (2000).

[6] Gallouet T., Hérard J.M., Seguin N., Some approximate Godunov schemes to compute shallow water equations with topography, *AIAA 2001*, (2000).

[7] Gerbeau J.F. and Perthame B., Derivation of viscous Saint-Venant system for laminar shallow water ; Numerical validation, *Discrete Cont. Dyn. Syst. Ser. B* (2001) 1, no. 1, 89-102.

[8] Godlewski E. and Raviart P.A., *Numerical approximation of hyperbolic systems of conservation laws*, Applied Mathematical Sciences **118**, New York, Springer-Verlag, 1996.

[9] Gosse L. and LeRoux A.Y., A well-balanced scheme designed for inhomogeneous scalar conservation laws, *C.R. Acad. Sci. Paris Sér.I Math.*, **323** (1996), no. 5, 543-546.

[10] Hervouet J.M., Hydrodynamique des écoulements à surface libre, apport de la méthode des élémants finis. EDF. (2001).

[11] Jin S., A steady state capturing method for hyperbolic system with geometrical source terms, *M2AN Math. Model. Numer. Anal.*, **35** (2001), 631-646.

[12] LeVêque R.J., *Numerical Methods for Conservation Laws. Second edition*, Lectures in Mathematics, ETH Zurich, Birkhauser, (1992).

[13] LeVêque R.J., Balancing source terms and flux gradients in high-resolution Godunov methods: the quasi-steady wave-propagation algorithm, *J. Comput. Phys.*, **146** (1998), no. 1, 346-365.

[14] Martin L., Fonctionnement écologique de la Seine à l'aval de la station d'épuration d'Achères : données expérimentales et modélisation bidimensionnelle, Phd thesis, Ecole des Mines de Paris, (2001).

[15] Perthame B., Kinetic formulations of conservation laws, Oxford University Press (2002).

[16] Perthame B. and Simeoni C., A kinetic scheme for the Saint-Venant system with a source term, *Calcolo*, **38** (2001), 201-231.

[17] Roe P.L., Upwind differencing schemes for hyperbolic conservation laws with source terms, *Nonlinear Hyperbolic Problems*, C.Carasso, P.A.Raviart and D.Serre editors, Lecture Notes in Math., vol. 1270, Berlin, Springer-Verlag, (1987), pp. 41-51.

[18] de Saint-Venant A.J.C., Théorie du mouvement non permanent des eaux, avec application aux crues de rivières et à l'introduction des marées dans leur lit, *C.R. Acad. Sc. Paris*, **73** (1871), 147-154.

[19] Stoker J.J., The formation of breakers and bores, *Com. on Appl. Math.*, Vol 1, No 1 (1948).

Contents

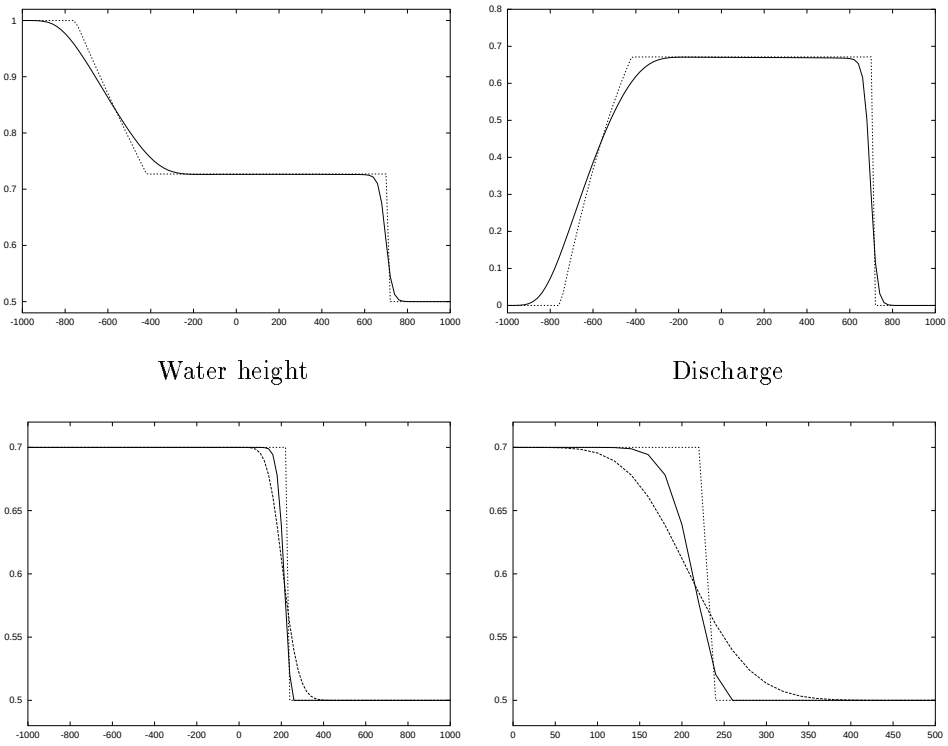

Figure 1: Dam break on a flat bottom : Hydrodynamic and pollutant

Two time steps scheme (continuous line)
Upwind scheme (dotted line)
Exact solution (small dotted line)

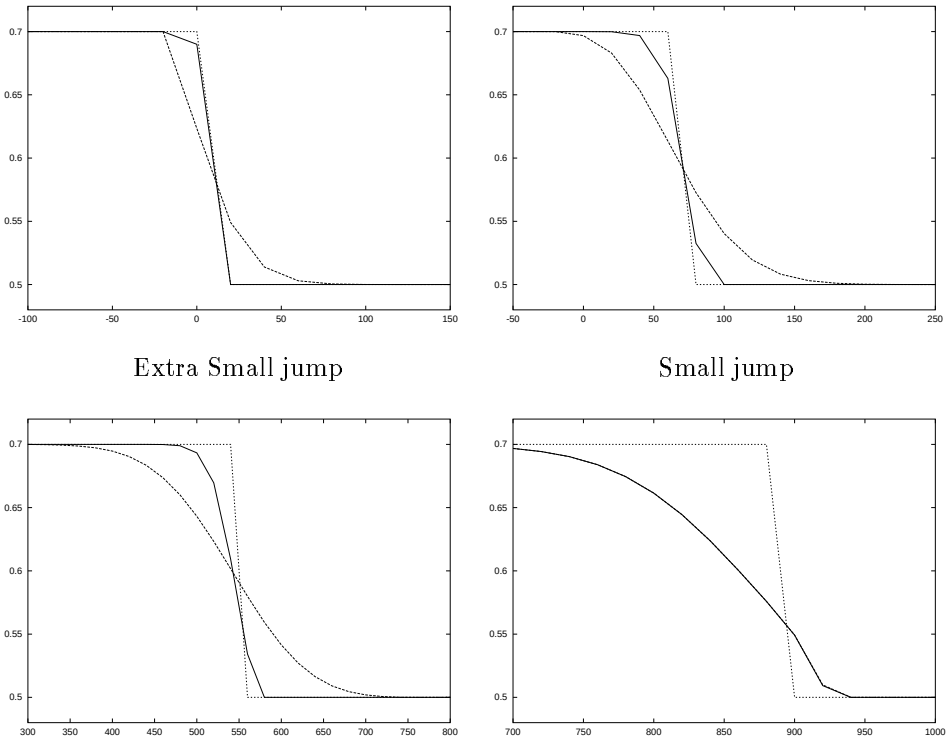

Extra Small jump

Small jump

Large jump

Extra large jump

Figure 2: Concentration of pollutant for some dam break problems

Two time steps scheme (continuous line)
Upwind scheme (dotted line)
Exact solution (small dotted line)

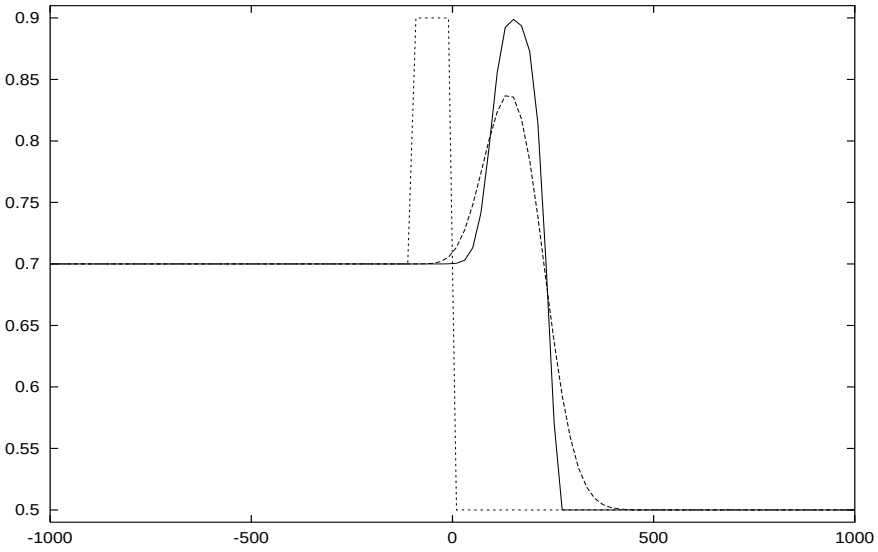

Figure 3: Concentration of pollutant for the peak problem

Two time steps scheme (continuous line)
Upwind scheme (dotted line)
Initial data (small dotted line)

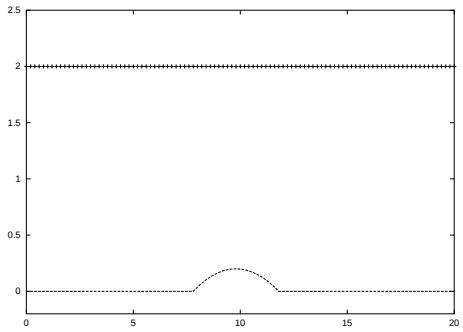

Water level profile
and bottom topography

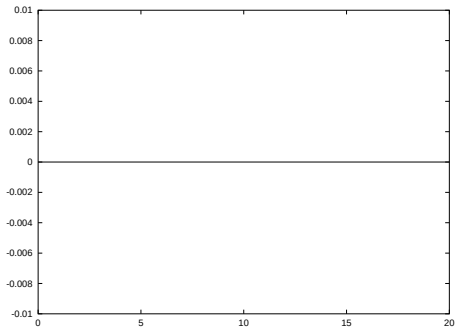

Discharge

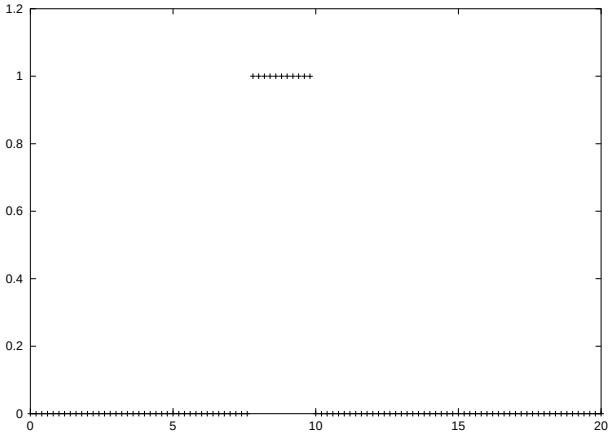

Concentration of pollutant

Figure 4: Lake at rest with polluted area

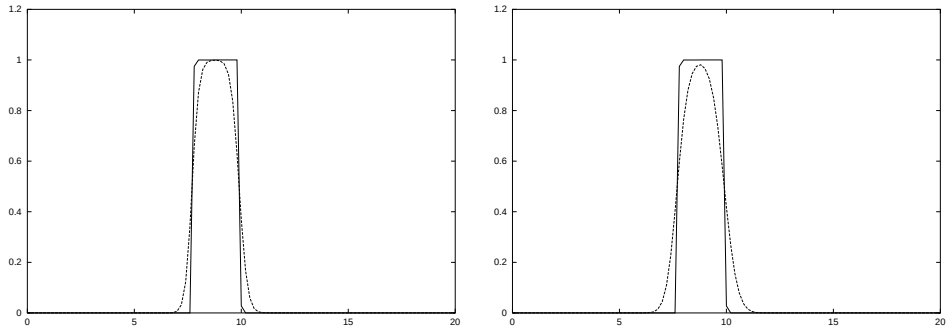

After one day After two days

Figure 5: Concentration of pollutant in a lake at rest after large time computation

Two time steps scheme (continuous line)
Upwind scheme (dotted line)

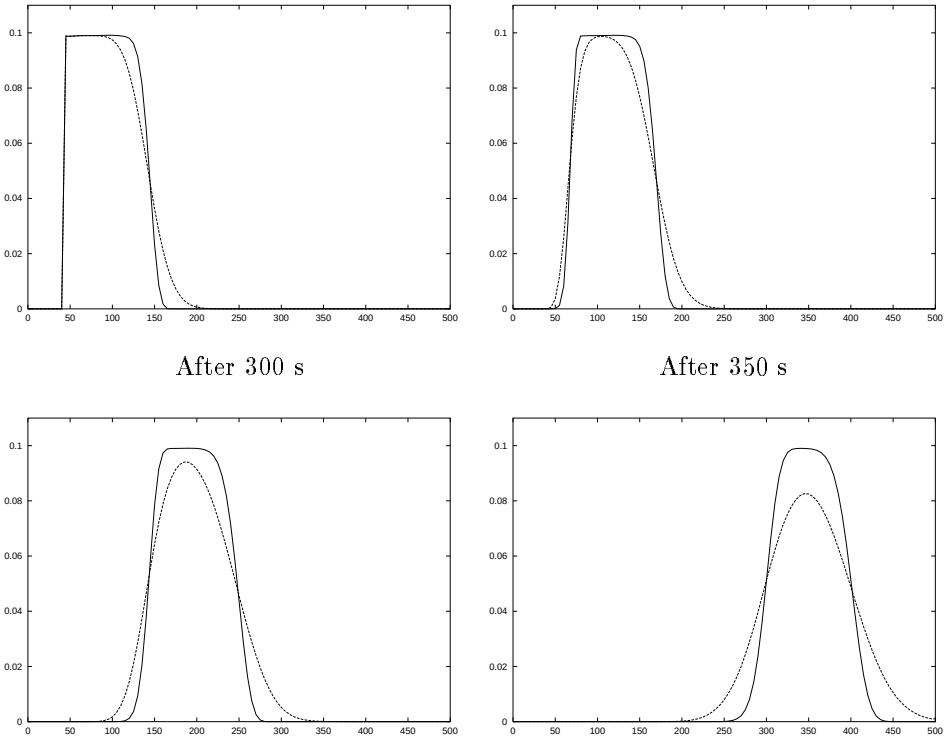

After 300 s

After 350 s

After 500 s

After 800 s

Figure 6: Emission of pollutant in a fluvial flow

Two time steps scheme (continuous line)
Upwind scheme (dotted line)

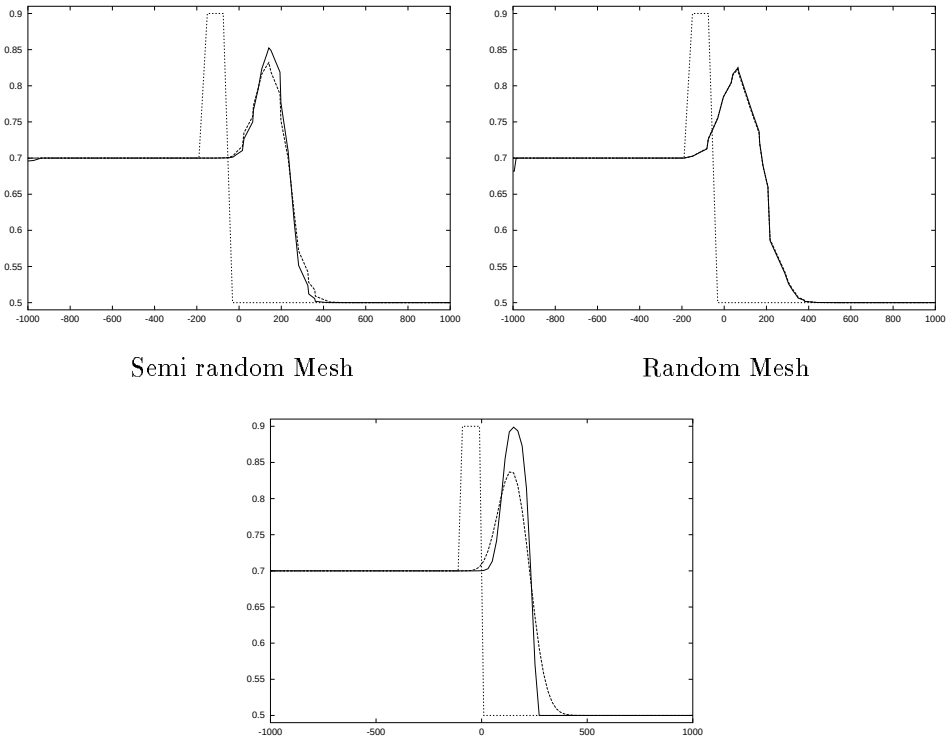

Semi random Mesh Random Mesh

Uniform Mesh

Figure 7: Concentration of pollutant for a peak problem with different meshes

Two time steps scheme (continuous line)
Upwind scheme (dotted line)
Initial data (small dotted line)

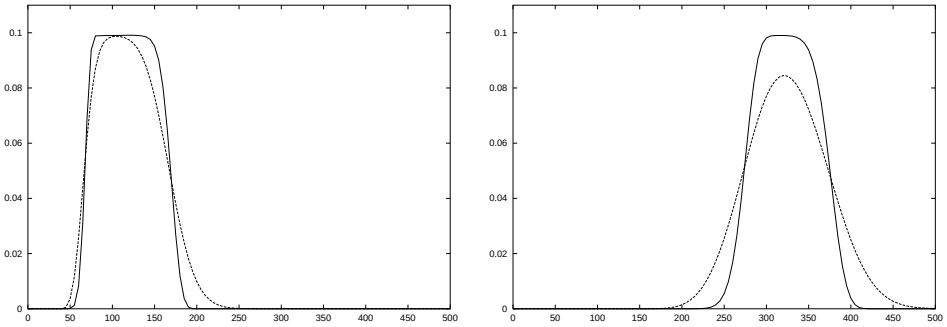

Uniform Mesh - 350s

Uniform Mesh - 750s

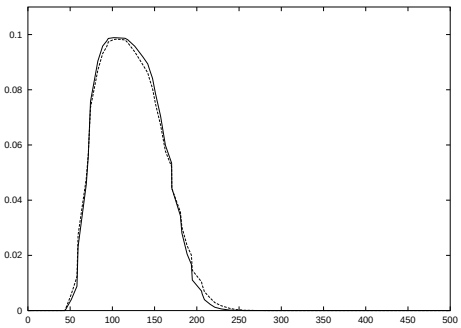

Semi random Mesh - 350s

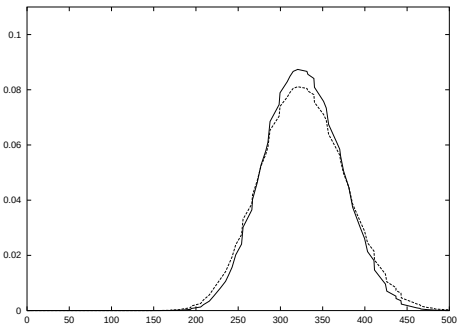

Semi random Mesh - 750s

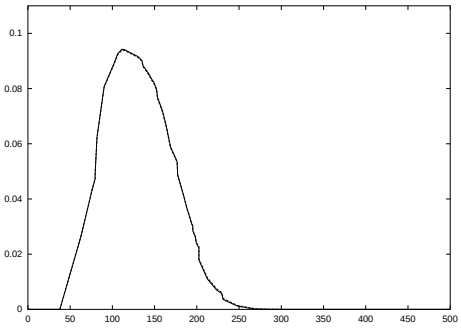

Random Mesh - 350s

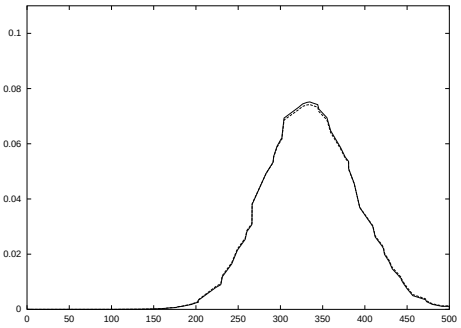

Random Mesh - 750s

Figure 8: Concentration of pollutant for an emission of pollutant problem with different meshes

Two time steps scheme (continuous line)
Upwind scheme (dotted line)

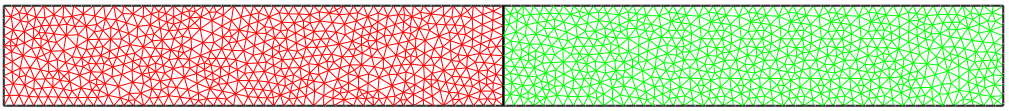

Unstructured mesh

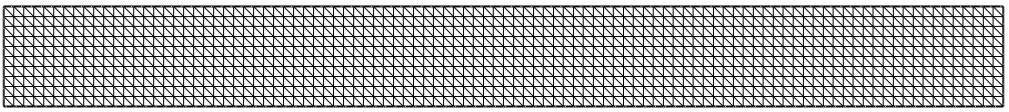

Uniform mesh

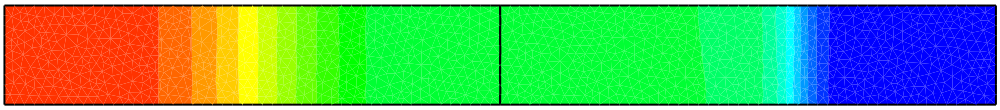

Water height

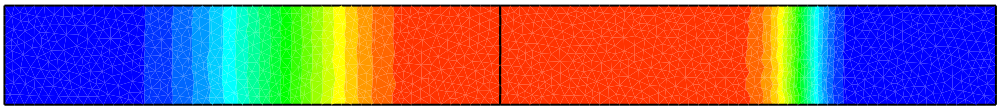

Froude Number

Figure 9: 2D dam break- Meshes and hydrodynamic results

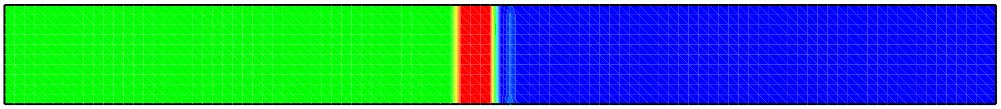

Initial solution

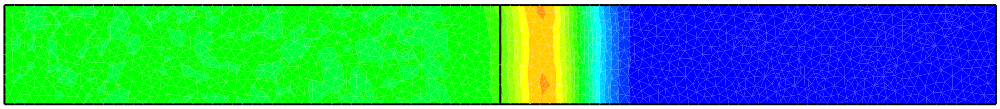

Unstructured mesh - Upwind kinetic scheme

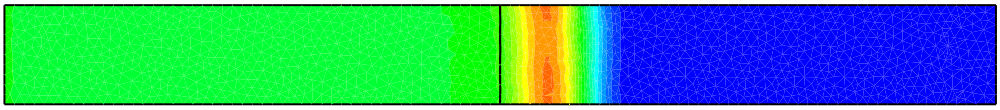

Unstructured mesh - Two time steps kinetic scheme

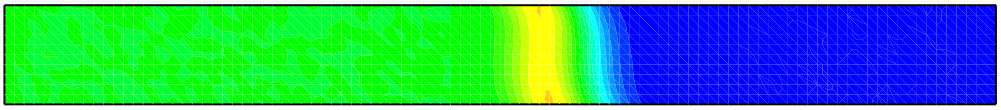

Uniform mesh - Upwind kinetic scheme

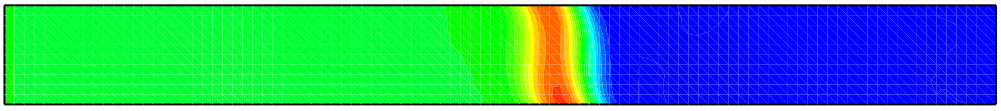

Uniform mesh - Two time steps kinetic scheme

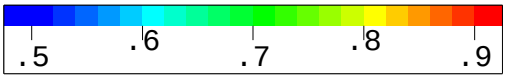

Scale for concentration of pollutant values

Figure 10: 2D dam break - Concentration of pollutant

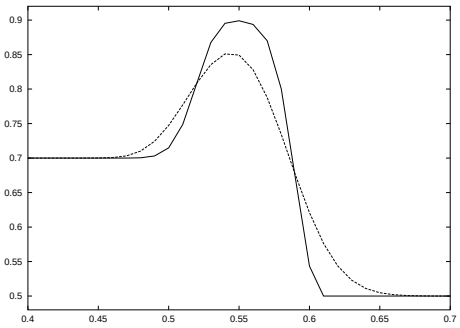

1D Uniform Mesh

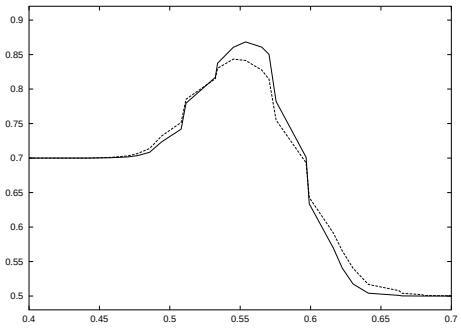

1D Semi random Mesh

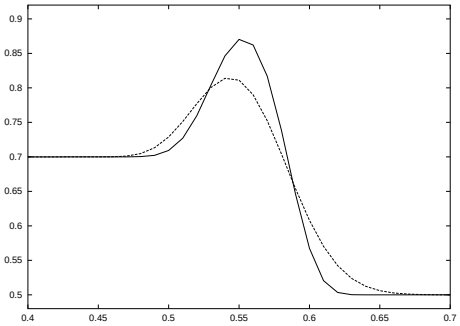

2D Uniform Mesh

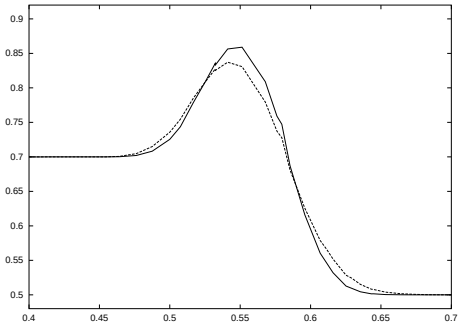

2D Irregular Mesh

Figure 11: Concentration of pollutant for a peak problem
Comparison between the 1D problem and the 2D problem (plane y=0.5)

Two time steps scheme (continuous line)
Upwind scheme (dotted line)

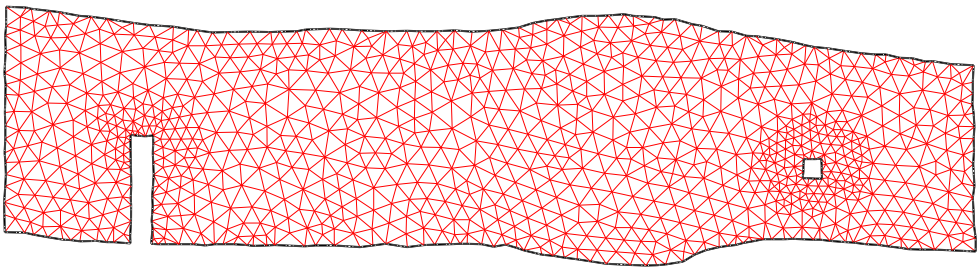

The mesh

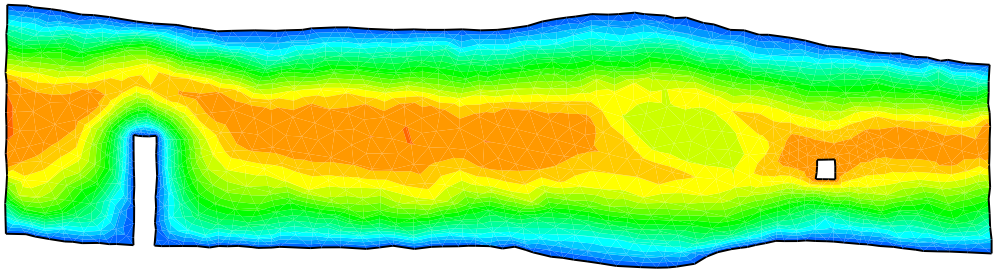

Water height

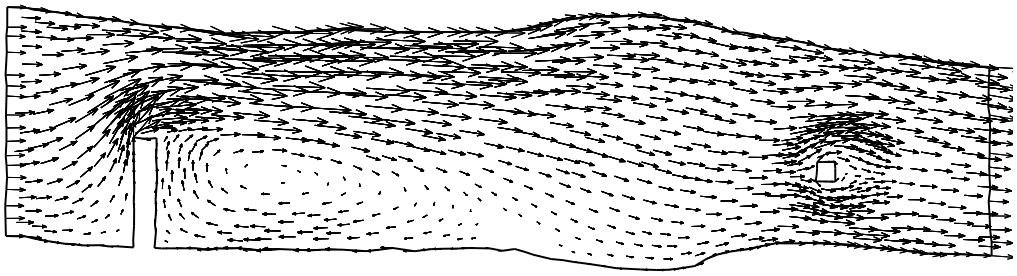

Velocity

Figure 12: River with emission of pollutant - Mesh and hydrodynamic results

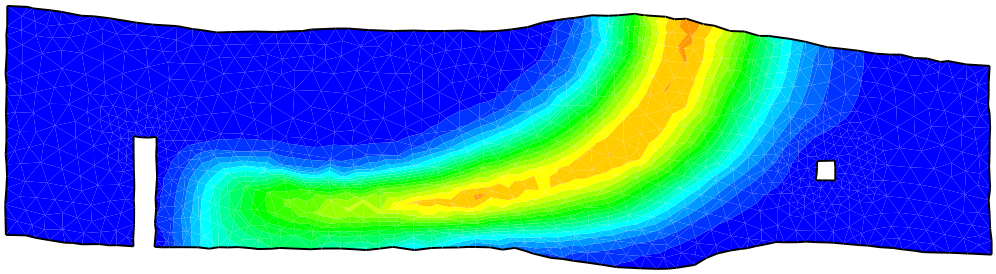

Concentration of pollutant - Upwind kinetic scheme

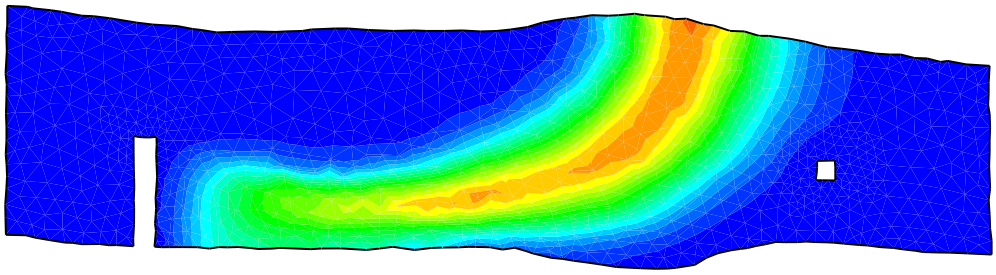

Concentration of pollutant - Two time steps kinetic scheme

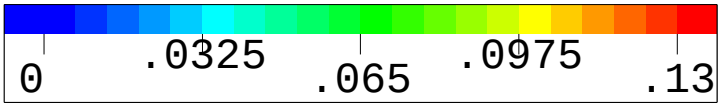

Scale for concentration of pollutant values

Figure 13: River with emission of pollutant - Concentration of pollutant

Unit de recherche INRIA Rocquencourt
Domaine de Voluceau - Rocquencourt - BP 105 - 78153 Le Chesnay Cedex (France)

Unit de recherche INRIA Lorraine : LORIA, Technople de Nancy-Brabois - Campus scientiøque
615, rue du Jardin Botanique - BP 101 - 54602 Villers-ls-Nancy Cedex (France)
Unit de recherche INRIA Rennes : IRISA, Campus universitaire de Beaulieu - 35042 Rennes Cedex (France)
Unit de recherche INRIA Rhne-Alpes : 655, avenue de l'Europe - 38330 Montbonnot-St-Martin (France)
Unit de recherche INRIA Sophia Antipolis : 2004, route des Lucioles - BP 93 - 06902 Sophia Antipolis Cedex (France)

diteur
INRIA - Domaine de Voluceau - Rocquencourt, BP 105 - 78153 Le Chesnay Cedex (France)
http://www.inria.fr
ISSN 0249-6399